Hybrid Materials Hot Paper

Deutsche Ausgabe: DOI: 10.1002/ange.201601611
Internationale Ausgabe: DOI: 10.1002/anie.201601611

Controlled Exfoliation of Layered Silicate Heterostructures into Bilayers and Their Conversion into Giant Janus Platelets

Matthias Stöter, Sebastian Gödrich, Patrick Feicht, Sabine Rosenfeldt, Herbert Thurn, Jens W. Neubauer, Maximilian Seuss, Peter Lindner, Hussein Kalo, Michael Möller, Andreas Fery, Stephan Förster, Georg Papastavrou, and Josef Breu**

Abstract: *Ordered heterostructures of layered materials where interlayers with different reactivities strictly alternate in stacks offer predetermined slippage planes that provide a precise route for the preparation of bilayer materials. We use this route for the synthesis of a novel type of reinforced layered silicate bilayer that is 15 % stiffer than the corresponding monolayer. Furthermore, we will demonstrate that triggering cleavage of bilayers by osmotic swelling gives access to a generic toolbox for an asymmetrical modification of the two vis-à-vis standing basal planes of monolayers. Only two simple steps applying arbitrary commercial polycations are needed to obtain such Janus-type monolayers. The generic synthesis route will be applicable to many other layered compounds capable of osmotic swelling, rendering this approach interesting for a variety of materials and applications.*

Exfoliation of layered compounds into two-dimensional nanosheets allows the tuning of phononic,[1] electronic,[2–5] ferroic,[6] electrochemical,[7] and mechanical properties.[8,9] Modulation of these properties is strongly related to the destruction or limitation of translational symmetry and is thus dependent on accurate control over the number of layers in the stacks.[10–12] Mono-, bi-, tri-, and multilayers must consequently be regarded as distinct phases. For example, bilayer phases of graphene and mica have been shown to have interesting electronic band structures.[4,13,14]

Various techniques ranging from epitaxial growth to mechanical exfoliation, potentially assisted by surface-active compounds or by rendering the starting material more shear labile by intercalation reactions, have been shown to yield two-dimensional (2D) materials. Established techniques, however, tend to produce broad distributions in the number of layers.[6,14–16]

Crystalline heterostructures with 1D-ordered structures along the stacking direction (also referred to as ordered or regularly interstratified compounds) are the thermodynamic equilibrium for many layered compounds intercalated with two different interlayer species that segregate into distinct interlayer spaces.[17–19] We recently established a general synthesis for such crystalline heterostructures composed of synthetic layered silicates (Figure 1 a).[19,20]

Herein, we prepare ordered heterostructures of layered silicates where interlayers with different reactivities strictly alternate in stacks. Such heterostructures offer predetermined slippage planes that provide a precise, scalable, and quantitative preparation route for desired bilayer materials.[5,21] The

[*] M. Stöter, P. Feicht, Dr. H. Kalo, Dr. M. Möller, Prof. Dr. J. Breu
Lehrstuhl für Anorganische Chemie I, University of Bayreuth
Universitätsstrasse 30, 95440 Bayreuth (Germany)
E-mail: Josef.Breu@uni-bayreuth.de

S. Gödrich, Prof. Dr. G. Papastavrou
Lehrstuhl für Physikalische Chemie II, University of Bayreuth
Universitätsstrasse 30, 95440 Bayreuth (Germany)
E-mail: georg.papastavrou@uni-bayreuth.de

Dr. S. Rosenfeldt, Prof. Dr. S. Förster
Lehrstuhl für Physikalische Chemie I, University of Bayreuth
Universitätsstrasse 30, 95440 Bayreuth (Germany)

H. Thurn
Computing Center, University of Bayreuth
Universitätsstrasse 30, 95440 Bayreuth (Germany)

J. W. Neubauer, M. Seuss, Prof. Dr. A. Fery
Institute for Physical Chemistry and Polymer Physics
Leibniz-Institut für Polymerforschung Dresden e.V.
01069 Dresden (Germany)

Dr. P. Lindner
Institut Laue-Langevin, DS LSS, 38042 Grenoble 9 (France)

Prof. Dr. A. Fery
Chair of Physical Chemistry of Polymeric Materials
Technical University Dresden, 01069 Dresden (Germany)

Supporting information for this article can be found under: http://dx.doi.org/10.1002/anie.201601611.

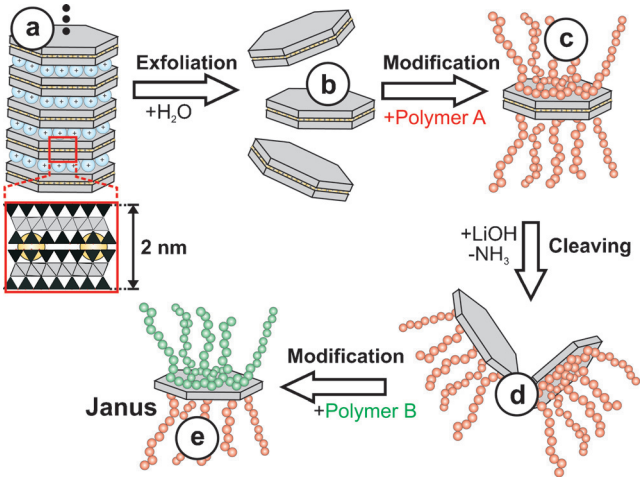

Figure 1. Selective swelling of a crystalline heterostructure (a) with NH_4^+ interlayers (yellow) and hydrated Na^+ interlayers (blue) induces highly selective exfoliation into bilayers (b). After external modification with a polycation A (red; c), modified bilayers can be cleaved under basic conditions using, for example, LiOH (d) while the symmetry is simultaneously broken at this stage. The platelets can be further modified (green) to form Janus-type platelets (e) with differently functionalized surfaces.

novel bilayers are significantly stiffer than monolayers, are at the same time easily cleavable and can be directly converted into Janus[22,23] platelets.

Synthetic sodium fluorohectorite ($Na_{0.5}^{inter}[Mg_{2.5}Li_{0.5}]^{oct}\langle Si_4\rangle^{tet}O_{10}F_2$) with typical lateral dimensions in the range of several micrometers (median ca. 20 μm)[24] is partially ion-exchanged with ammonium cations (NH_4^+) to yield a crystalline heterostructure (Supporting Information, Figure S1).

When NH_4^+ and Na^+ are chosen as the segregated interlayer cation pair, alternating NH_4^+ interlayers are formed, which do not hydrate, while adjacent Na^+ interlayers readily hydrate (Supporting Information, Figures S1 and S2).

In an intercalation compound of charged host layers, interlayer cations of different size will always be forced to segregate into different interlayers with densely packed structures since this allows for minimizing the average d-spacing and therefore maximizing the Coulomb energy. The cation density in a particular type of interlayer does not necessarily have to match the charge density of the layered silicate host if a local charge balance is assured by adjusting the second type of interlayer accordingly.[19,20] In our case, the NH_4^+ interlayers are significantly above while the Na^+ interlayers are below the charge density of the host layers (Supporting Information, Figure S1). As evidenced by equilibration experiments, the formation of ordered heterostructures is thermodynamically favored.[19,20]

In deionized water, Na^+ interlayers swell osmotically, which means that at the early swelling states all available water is drawn into the Na^+ interlayers. In the obtained Wigner crystal phase, the distance between the NH_4^+-bridged bilayers corresponds to the silicate to water ratio (Supporting Information, Figure S3). By adding increasing amounts of water, the separation steadily increases (Figure 2) to the point where the bilayers gain rotational freedom and the layer separation is consequently no longer determined by the volume ratio of silicate layer to water.

Osmotic swelling is the most gentle exfoliation method, and therefore the large platelet diameters are preserved.[25] Thus, by simply suspending these crystalline heterostructures in water, bilayers with extremely high aspect ratios up to 8000 are produced with unprecedented precision (Figure 1b; Supporting Information, Figures S4, S9, S10).

Quantitative and selective bilayer formation is proven by small angle X-ray scattering (SAXS) studies of the highly swollen heterostructured sample (Figure 2, gray trace).

The SAXS pattern scales in the low q range as q^{-2}, which is typically observed for platelet shaped scattering objects. At a solid content of 4 wt%, for instance, the bilayers of the exfoliated heterostructure are uniformly separated to 59 nm. The first form factor minimum appears around $q = 0.26$ Å^{-1}, followed by a second minimum around $q = 0.76$ Å^{-1}. We use a very simplified SAXS model of discs with homogeneous electron density to fit the experimental data (see the Supporting Information for further details), rendering the minima somewhat shallow.

The best fit for the SAXS trace is obtained with a bilayer thickness of 2.1 nm. This value corresponds to the sum of two silicate layers of 0.85 nm and an interlayer height of 0.4 nm.

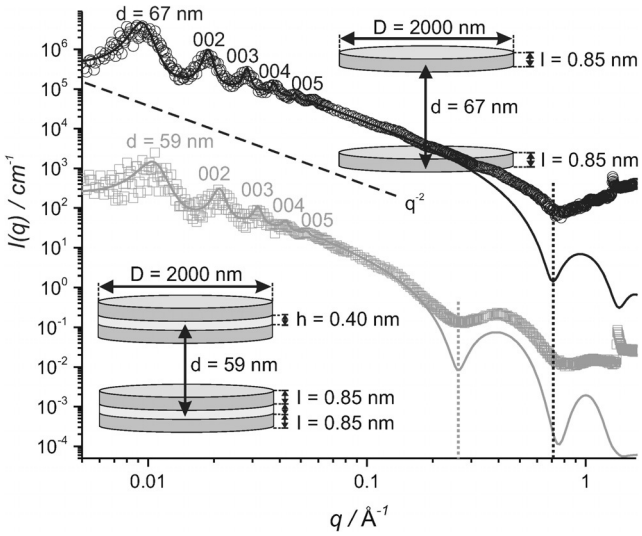

Figure 2. SAXS results of swollen gel samples (4 wt%): pristine bilayer sample (gray □) and a sample after cleaving with LiOH (black ○). The intensities of the cleaved sample are shifted by a factor of 10000 to avoid overlap. The corresponding solid lines are fits with a model of bilayer discs and single discs (see schemes and Supporting Information for further details). The dotted lines mark the position of the first minima of the form factors for bilayers (gray) and after cleavage to monolayers by the addition of LiOH (black). The scaling of q for the low q-range is indicated by a dashed line.

Bilayer formation is further confirmed by atomic force microscopy (AFM) of a sample obtained by drying a highly diluted, isotropic sol where platelets with a thickness of 2.6 nm are detected (Supporting Information, Figure S4).

Shih et al.[5] were the first to propose a route for the synthesis of bi- and trilayers of graphene starting with ionic stage-two and stage-three ICl or IBr intercalates of graphene. These graphite intercalates are popped by shock expansion, but they are unable to swell in solvents. Consequently, they lack an appropriate route for subsequent gentle and highly selective exfoliation. Moreover, the transformation of bilayers into Janus platelets, as described below, requires a second quantitative cleavage of bilayers via osmotic swelling.

Our novel silicate bilayers can easily be converted into monolayers by using bases to deprotonate the NH_4^+ cations; these cations hold the silicate layers together. Treating the suspension of bilayers with LiOH initially exchanges NH_4^+ with Li^+. Then, the bilayers are quantitatively cleaved by osmotic swelling of the resulting Li^+ interlayers into singular silicate layers (Figure 2, black trace). In the SAXS pattern, the first form factor minimum of the single layer sample shifts from $q = 0.26$ Å^{-1}, as observed for the bilayer, to $q = 0.73$ Å^{-1} (Figure 2). The best fit for the SAXS trace is obtained with a single layer thickness of 0.85 nm.

Owing to the collapse of the NH_4^+ interlayer, the structure of the bilayer is comparable to the bonding situation in potassium-rich micas: the NH_4^+ cations inside the collapsed interlayer space will protrude on both sides into the hexagonal cavities of the Kagome-like silicate surface, cross-linking the two silicate layers encompassing this single interlayer space in the bilayer (Figure 3c). The bilayer may be regarded

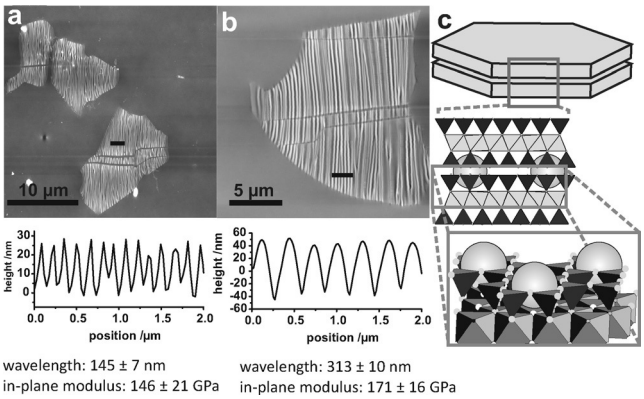

Figure 3. Determination of the in-plane bending moduli: Typical AFM topographical images of wrinkled a) monolayers and b) bilayers on PDMS substrates. The corresponding height profiles (black bars) are shown below. The resulting wavelength and in-plane modulus are obtained by Fourier transformation. c) The structure of a reinforced bilayer-sandwich. NH_4^+ cations (gray ○) protrude into the upper and lower hexagonal cavities of the silicate surface (additional details are shown in the Supporting Information, Figures S6, S7).

as a nanosandwich structure; therefore, it is expected to be stiffer than a single lamella.[26,27] When comparing the in-plane moduli of a single layer and a bilayer, the latter is indeed found to be 15% stiffer (Figure 3). The in-plane moduli of a single layer and a bilayer were determined by a supported metrology using a simple wrinkling technique in which the observed wavelength is directly related to the in-plane modulus of the platelet (see Figure S6 and Figure S7 and the more detailed explanation in the Supporting Information).[9,26] The in-plane modulus of a single lamellae is found to be 146 ± 21 GPa, which is in good agreement with previous results.[26] The average in-plane modulus of the bilayer, however, is significantly higher and was determined to be 171 ± 16 GPa. Interestingly, the value of the bilayer is already in the range of the in-plane moduli of bulk mica (178.5 ± 1.5 GPa) as determined by conventional methods.[26,28,29]

The base lability of the NH_4^+ interlayer allows for the quantitative conversion of bilayers into Janus-type nanoplatelets. The importance and prospective applications of Janus particles was first noted by de Gennes.[30] Distinct chemical and physical properties of the basal surfaces of Janus platelets offer directionality, allowing complex self-assembly.[23] Many approaches to synthesize inorganic–organic Janus particles were developed.[31–33] Typically the symmetry of inorganic particles is broken by immobilization of the particles at the surface of templates or interfaces followed by selective modification of one hemisphere of the particle.[34–36]

When starting with the bilayers described herein, breaking symmetry is beautifully simple (Figure 1d). Janus character can be directly realized by selectively coating the two surfaces of the monolayers with different polymers: Commercial polyethyleneimine-ethyleneoxide (PEI-EO) and the dendritic poly(amidoamine) of generation G10 yield morphologically different monolayers that can be distinguished clearly by AFM imaging. Such Janus platelets are made by first coating both surfaces of the bilayer by PEI-EO. Then, the bilayers are cleaved, and the produced Li^+-decorated (Figure 1d) surfaces are "stained" with PAMAM G10 (Figure 1e), which does not adsorb to the PEI-EO-terminated surfaces. The irreversible exchange[37] of the Na^+ cations and the uniform coating of both surfaces of the bilayers with PEI-EO (Figure 1c) was probed by small-angle neutron scattering (SANS; Supporting Information, Figure S8). The overall thickness of the modified bilayer increases to 5.8 nm upon cation exchange with PEI-EO. As expected, after cleavage, SANS indicates a Janus platelet thickness of 3 nm (Figure 1d), which corresponds to a 1 nm-thick silicate layer coated on one side with an approximately 2 nm-thick monolayer of PEI-PEO (see the Supporting Information).

As already mentioned, the Li^+-decorated surface is subsequently exchanged by PAMAM G10, which is known to bind quasi-irreversibly to negatively charged surfaces.[38,39] The adsorption process follows the random sequential adsorption (RSA) model and leads to a fractional surface coverage.[38] For sufficiently large dendrimers (> G5), single dendrimers can be readily resolved by AFM. Moreover, PAMAM G10 has a very narrow M_W distribution, which results in nearly identical heights and diameters of the adsorbed dendrimers. Hence, the surface morphology is easily distinguishable from the smooth PEI-EO covered surface (Figure 4a).

AFM samples were prepared by aspiration onto micropore filters (Figure 4a), which produces some degree of aggregation of individual platelets but suppresses any preferred orientation of the Janus platelets. The extremely high aspect ratios always force the platelets into orientations parallel to the substrate (Figure 4b and c), but the distinct surfaces are randomly exposed up or down.

The AFM signal corresponding to the adhesion shows two distinct types of surface morphologies for individual platelets: one with very high dendrimer coverage and one with negligible dendrimer coverage (Figure 4d and e). This difference in adhesion corresponds to the two different surface types of the Janus platelets: PAMAM or PEI-EO. The coverage of the platelets with very high dendrimer content (Figure 4e) resembles the level of dendrimer coverage of the bilayers that were modified with PAMAM for comparison (Supporting Information, Figure S9). As expected, dendrimer adsorption to the negatively charged silicate layers follows the RSA model.[38] The presence of two distinct surfaces in terms of dendrimer coverage unequivocally confirms the selective modification of the platelets in an asymmetric manner and thus the preparation of Janus-type platelets.

In conclusion, a novel approach for a quantitative, cost-effective, and robust fabrication of mechanically reinforced bilayers via osmotic exfoliation of ordered heterostructures is established. The synthesis route for bilayers will be generally applicable to other layered compounds capable of osmotic swelling, such as layered titanates, niobates, or perovskites.[40–44] By cleaving bilayers with appropriate reagents, in this case bases, the symmetry is broken in the simplest way, giving access to a general method for the synthesis of asymmetrically modified Janus nanoplatelets with tuneable functionalities.

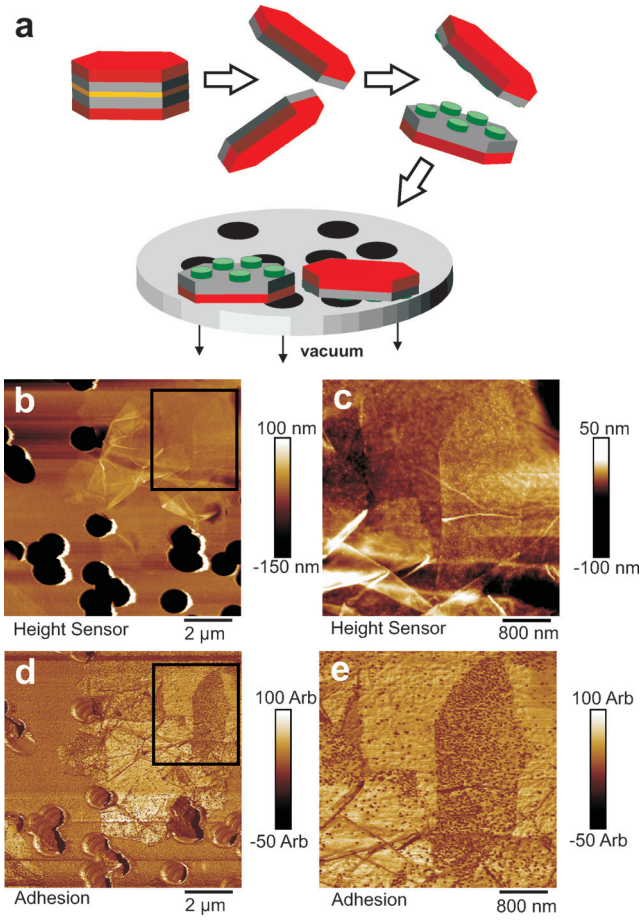

Figure 4. a) The Janus modification of the nanoplatelets. PEI-EO-modified bilayers were cleaved, and new Li^+-decorated surfaces are subsequently modified with dendrimers, which serve as tracers for AFM imaging. The Janus platelets are immobilized onto a micropore filter by vacuum filtration. The AFM images of the topography (b, c) and adhesion (d, e) of the Janus platelets show different surface morphologies and adhesion properties. In particular, the adhesion signals unequivocally enable the identification of distinct surfaces with negligible and high dendrimer coverage, respectively. The Janus platelets are randomly oriented. Consequently, digital magnification (d, e) demonstrates that dendrimers are present only on such platelets, exposing this surface type to the AFM. More high-resolution images can be found in the Supporting Information, Figures S9–S11.

Acknowledgements

This work was financially supported by the Deutsche Forschungsgemeinschaft (SFB 840). Andreas Schedl is gratefully acknowledged for helping with the PDMS tensile tests.

Keywords: atomic force microscopy · hybrid materials · nanomaterials · silicate · thin layers

How to cite: *Angew. Chem. Int. Ed.* **2016**, *55*, 7398–7402
Angew. Chem. **2016**, *128*, 7524–7528

[1] C. Chiritescu, D. G. Cahill, N. Nguyen, D. Johnson, A. Bodapati, P. Keblinski, P. Zschack, *Science* **2007**, *315*, 351–353.
[2] K. Takada, H. Sakurai, E. Takayama-Muromachi, F. Izumi, R. A. Dilanian, T. Sasaki, *Nature* **2003**, *422*, 53–55.
[3] K. S. Novoselov, A. K. Geim, S. V. Morozov, D. Jiang, Y. Zhang, S. V. Dubonos, I. V. Grigorieva, A. A. Firsov, *Science* **2004**, *306*, 666–669.
[4] M. Sui, G. Chen, L. Ma, W. Y. Shan, D. Tian, K. Watanabe, T. Taniguchi, X. Jin, W. Yao, D. Xiao, Y. Zhang, *Nat. Phys.* **2015**, *11*, 1027–1031.
[5] C. J. Shih, A. Vijayaraghavan, R. Krishnan, R. Sharma, J. H. Han, M. H. Ham, Z. Jin, S. C. Lin, G. L. C. Paulus, N. F. Reuel, Q. H. Wang, D. Blankschtein, M. S. Strano, *Nat. Nanotechnol.* **2011**, *6*, 439–445.
[6] W. Wu, L. Wang, Y. Li, F. Zhang, L. Lin, S. Niu, D. Chenet, X. Zhang, Y. Hao, T. F. Heinz, J. Hone, Z. L. Wang, *Nature* **2014**, *514*, 470–474.
[7] O. Mashtalir, M. Naguib, V. N. Mochalin, Y. Dall'Agnese, M. Heon, M. W. Barsoum, Y. Gogotsi, *Nat. Commun.* **2013**, *4*, 1716.
[8] J. W. Suk, R. D. Piner, J. An, R. S. Ruoff, *ACS Nano* **2010**, *4*, 6557–6564.
[9] D. A. Kunz, P. Feicht, S. Goedrich, H. Thurn, G. Papastavrou, A. Fery, J. Breu, *Adv. Mater.* **2013**, *25*, 1337–1341.
[10] B. Rasche, A. Isaeva, M. Ruck, S. Borisenko, V. Zabolotnyy, B. Buchner, K. Koepernik, C. Ortix, M. Richter, J. van den Brink, *Nat. Mater.* **2013**, *12*, 422–425.
[11] B. V. Lotsch, G. A. Ozin, *Adv. Mater.* **2008**, *20*, 4079–4084.
[12] S. H. Yu, M. Antonietti, H. Colfen, M. Giersig, *Angew. Chem. Int. Ed.* **2002**, *41*, 2356–2360; *Angew. Chem.* **2002**, *114*, 2462–2466.
[13] T. Ohta, A. Bostwick, T. Seyller, K. Horn, E. Rotenberg, *Science* **2006**, *313*, 951–954.
[14] S. S. Kim, T. Van Khai, V. Kulish, Y. H. Kim, H. G. Na, A. Katoch, M. Osada, P. Wu, H. W. Kim, *Chem. Mater.* **2015**, *27*, 4222–4228.
[15] B. Butz, C. Dolle, F. Niekiel, K. Weber, D. Waldmann, H. B. Weber, B. Meyer, E. Spiecker, *Nature* **2014**, *505*, 533–537.
[16] M. Lotya, Y. Hernandez, P. J. King, R. J. Smith, V. Nicolosi, L. S. Karlsson, F. M. Blighe, S. De, Z. M. Wang, I. T. McGovern, G. S. Duesberg, J. N. Coleman, *J. Am. Chem. Soc.* **2009**, *131*, 3611–3620.
[17] W. L. Ijdo, T. Lee, T. J. Pinnavaia, *Adv. Mater.* **1996**, *8*, 79–83.
[18] W. L. Ijdo, T. J. Pinnavaia, *J. Solid State Chem.* **1998**, *139*, 281–289.
[19] M. W. Möller, D. Hirsemann, F. Haarmann, J. Senker, J. Breu, *Chem. Mater.* **2010**, *22*, 186–196.
[20] M. Stöter, B. Biersack, N. Reimer, M. Herling, N. Stock, R. Schobert, J. Breu, *Chem. Mater.* **2014**, *26*, 5412–5419.
[21] M. Stöter, B. Biersack, S. Rosenfeldt, M. J. Leitl, H. Kalo, R. Schobert, H. Yersin, G. A. Ozin, S. Förster, J. Breu, *Angew. Chem. Int. Ed.* **2015**, *54*, 4963–4967; *Angew. Chem.* **2015**, *127*, 5047–5051.
[22] A. Walther, X. Andre, M. Drechsler, V. Abetz, A. H. E. Muller, *J. Am. Chem. Soc.* **2007**, *129*, 6187–6198.
[23] A. Walther, A. H. E. Müller, *Chem. Rev.* **2013**, *113*, 5194–5261.
[24] M. Stöter, D. A. Kunz, M. Schmidt, D. Hirsemann, H. Kalo, B. Putz, J. Senker, J. Breu, *Langmuir* **2013**, *29*, 1280–1285.
[25] M. Stöter, S. Rosenfeldt, J. Breu, *Annu. Rev. Mater. Res.* **2015**, *45*, 129–151.
[26] D. A. Kunz, J. Erath, D. Kluge, H. Thurn, B. Putz, A. Fery, J. Breu, *ACS Appl. Mater. Interfaces* **2013**, *5*, 5851–5855.
[27] M. W. Möller, U. A. Handge, D. A. Kunz, T. Lunkenbein, V. Altstadt, J. Breu, *ACS Nano* **2010**, *4*, 717–724.
[28] G. D. Zartman, H. Liu, B. Akdim, R. Pachter, H. Heinz, *J. Phys. Chem. C* **2010**, *114*, 1763–1772.
[29] A. Castellanos-Gomez, M. Poot, A. Amor-Amoros, G. A. Steele, H. S. J. van der Zant, N. Agrait, G. Rubio-Bollinger, *Nano Res.* **2012**, *5*, 550–557.
[30] P. G. de Gennes, *Science* **1992**, *256*, 495–497.
[31] D. Hirsemann, S. Shylesh, R. A. De Souza, B. Diar-Bakerly, B. Biersack, D. N. Müller, M. Martin, R. Schobert, J. Breu, *Angew.*

Chem. Int. Ed. **2012**, *51*, 1348 – 1352; *Angew. Chem.* **2012**, *124*, 1376 – 1380.
[32] C. Ma, H. Wu, Z. H. Huang, R. H. Guo, M. B. Hu, C. Kubel, L. T. Yan, W. Wang, *Angew. Chem. Int. Ed.* **2015**, *54*, 15699 – 15704; *Angew. Chem.* **2015**, *127*, 15925 – 15930.
[33] W. O. Yah, A. Takahara, Y. M. Lvov, *J. Am. Chem. Soc.* **2012**, *134*, 1853 – 1859.
[34] J. H. Liu, G. N. Liu, M. M. Zhang, P. C. Sun, H. Y. Zhao, *Macromolecules* **2013**, *46*, 5974 – 5984.
[35] F. X. Liang, K. Shen, X. Z. Qu, C. L. Zhang, Q. A. Wang, J. L. Li, J. G. Liu, Z. Z. Yang, *Angew. Chem. Int. Ed.* **2011**, *50*, 2379 – 2382; *Angew. Chem.* **2011**, *123*, 2427 – 2430.
[36] L. M. Zhang, J. W. Yu, M. M. Yang, Q. Xie, H. L. Peng, Z. F. Liu, *Nat. Commun.* **2013**, *4*, 1443.
[37] M. Ziadeh, S. Weiss, B. Fischer, S. Förster, V. Altstädt, A. H. Müller, J. Breu, *J. Colloid Interface Sci.* **2014**, *425*, 143 – 151.
[38] R. Pericet-Camara, G. Papastavrou, M. Borkovec, *Langmuir* **2004**, *20*, 3264 – 3270.
[39] B. P. Cahill, G. Papastavrou, G. J. M. Koper, M. Borkovec, *Langmuir* **2008**, *24*, 465 – 473.
[40] Y. Ebina, T. Sasaki, M. Watanabe, *Solid State Ionics* **2002**, *151*, 177 – 182.
[41] F. Geng, R. Ma, A. Nakamura, K. Akatsuka, Y. Ebina, Y. Yamauchi, N. Miyamoto, Y. Tateyama, T. Sasaki, *Nat. Commun.* **2013**, *4*, 1632.
[42] M. Osada, G. Takanashi, B. W. Li, K. Akatsuka, Y. Ebina, K. Ono, H. Funakubo, K. Takada, T. Sasaki, *Adv. Funct. Mater.* **2011**, *21*, 3482 – 3487.
[43] T. Sasaki, M. Watanabe, *J. Am. Chem. Soc.* **1998**, *120*, 4682 – 4689.
[44] Y. J. Song, N. Iyi, T. Hoshide, T. C. Ozawa, Y. Ebina, R. Z. Ma, N. Miyamoto, T. Sasaki, *Chem. Commun.* **2015**, *51*, 17068 – 17071.

Received: February 15, 2016
Revised: March 24, 2016
Published online: May 3, 2016

